İSTANBUL UNIVERSITY CERRAHPAŞA

ORIGINAL ARTICLE
Electrica 2024; 24(1): 163-174

Sensitivity Analyses for All-Dielectric Absorber Structures Having Different Dielectric Resonator Geometries and Investigation of the Effect of Boundary Conditions on the Absorption Spectra

Nezihe Karacan[1], Gönül Turhan-Sayan[2], Evren Ekmekçi[1]

[1]Department of Electrical and Electronics Engineering, Süleyman Demirel University, Faculty of Engineering and Natural Sciences, Isparta, Turkey
[2]Department of Electrical and Electronics Engineering, Middle East Technical University, Faculty of Engineering, Ankara, Turkey

Cite this article as: N. Karacan, G. Turhan-Sayan and E. Ekmekçi, "Sensitivity analyses for all-dielectric absorber structures having different dielectric resonator geometries and investigation of the effect of boundary conditions on the absorption spectra," *Electrica*, 24(1), 163-174, 2024.

ABSTRACT

In this study, several performance analyses are conducted on all-dielectric absorbers composed of cylindrical-, elliptical-, square-, rectangular-, hexagonal-, and octagonal-shaped dielectric resonators. These performance analyses include the numerical investigation of the change in the resonance frequency and the absorption peak level with respect to the changes in dielectric constant and loss tangent, respectively, in the WR-284 rectangular waveguide setup. In addition, the designed structures are also analyzed in a free-space simulation setup to present the differences that come from using different boundary conditions and excitations. The analyses reveal that the absorption spectra behaviors are similar in response to changes in dielectric constants and loss tangents among the studied geometries. Absorption peak levels of the observed higher-order resonance modes are highly dependent on the resonator geometry. On the other hand, the free-space simulation results reveal that the designed structures have negligible cross-polarization components, hence they do not practically contribute to the absorption spectra. Moreover, absorption, reflection, and transmission spectra are highly affected by differences in the simulation setup and accordingly by the excitation signal for all resonator geometries. In addition, behavior of the absorption spectra for all the dielectric resonator geometries are investigated under the oblique incident wave for TE and TM modes. It has been noticed that the absorption spectra are nearly independent of the angle at lower incident angle values. It is believed that these analyses will contribute to the sensor studies based on all-dielectric absorber designs.

Index Terms— Absorption, all-dielectric absorber, dielectric resonator geometry, effect of boundary conditions, sensitivity.

I. INTRODUCTION

At the beginning of the 20th century, it was put forward by R. D. Richtmyer that appropriately sized objects having high dielectric constants could be used as dielectric resonators (DRs) [1]. Recently, DRs have become a popular research topic due to their physical advantages, such as being easily integrated into the circuit owing to their compact sizes [2, 3], enduring oxidation and corrosion, and presenting high operating stability at high temperatures [4, 5]. In addition, since the various resonance modes (electric dipoles, magnetic dipoles, quadrupoles and octupoles, etc.) are supported inside the dielectric resonators [3], the dielectric resonators possess wide application fields from microwave to optical frequency regions [4-21]. In literature, DRs are used in diverse applications such as antenna [6, 7, 11], filter [4], electromagnetically induced transparency [8], [15], absorber [5, 9, 12, 13, 17-21], polarizer [14], and sensor designs [7, 12, 13, 16-21].

In the literature, although the studies based on cylindrical-shaped [3-6, 8, 10, 11, 13, 18, 21] dielectric resonator (DR) designs are common, there are also studies with elliptical- [14, 21], hemispheric- [7], conical- [22], square- [10, 17, 20-22], rectangular- [3, 6, 11, 16, 21], hexagonal- [6, 21], octagonal- [6, 21], triangular- [10], and pentagonal-shaped [10] resonator geometries. However, the number of studies investigating the effects of resonator geometry on transmission, reflection, or absorption spectra is relatively limited [6, 9, 10, 11, 12]. In more detail, Meher et al. performed antenna designs using cylindrical-, rectangular-, hexagonal-, and octagonal-shaped DRs and investigated the effects of resonator geometry on the antenna parameters such as gain, directivity, and bandwidth [6]. Zhao et al. designed broadband absorber structures with droplet- and tube-shaped resonators composed of water as

Corresponding author:
Evren Ekmekçi

E-mail:
evrenekmekci@sdu.edu.tr

Received: May 6, 2023

Revision Requested: June 12, 2023

Accepted: October 5, 2023

Publication Date: January 31, 2024

DOI: 10.5152/electrica.2024.23064

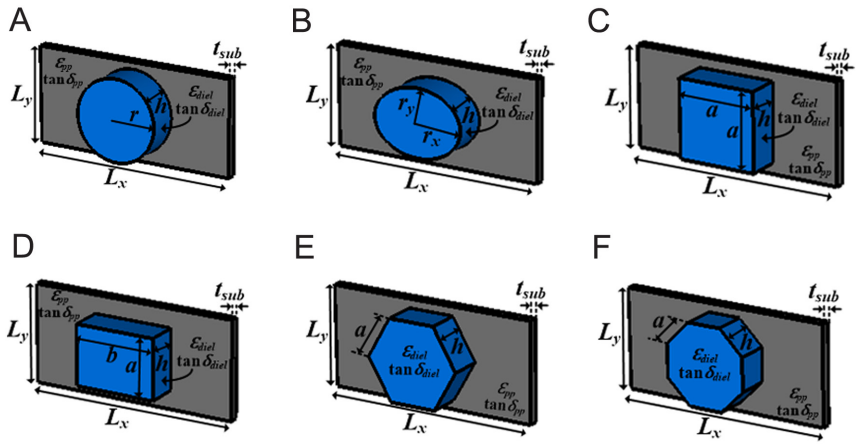

Fig. 1. (a) to (f) The schematics and the design parameters of designed all-dielectric absorbers with (a) cylindrical-, (b) elliptical-, (c) square-, (d), rectangular-, (e) hexagonal-, and (f) octagonal-shaped DRs.

the dielectric material and investigated the effects of the absorber designs on the absorption level and the absorption bandwidth [9]. Seo et al. designed triangular-, square-, pentagonal-, hexagonal-, octagonal-, cylindrical-, and cross-shaped resonator structures and investigated the effects of the DR geometry on high transmission and full phase control in the THz region comparatively [10]. Whiting et al. studied DR antenna designs with various geometries based on superformula and shape optimization and presented the effects of the resonator geometry on antenna radiation parameters [11]. Zhao and Cheng designed an all-dielectric absorber using a micro-cross-shaped resonator with the temperature-sensitive strontium titanate (STO) material and analyzed the absorption performance for the changing temperature of STO. In addition, they have demonstrated that the THz perfect absorption can also be obtained with the square, cylindrical, and ring dielectric resonator structures using the STO material [12].

There are studies in the literature studying on the effects of dielectric constant (ε_{diel}) and dielectric loss tangent ($\tan\delta_{diel}$) of the DR on the sensitivity for a single DR geometry [7, 13, 16-20]. In more detail, Wang et al. investigated the effects of change in the dielectric properties, which was controlled by temperature, on the reflection spectrum on a rectangular-shaped DR made of temperature-sensitive calcium titanate material [16]. Jacobsen et al. designed an antenna with a hemispherical DR made of water and observed the change on reflection spectra in response to change in the dielectric properties of water depending on the temperature [7]. Karacan and Ekmekci presented an all-dielectric absorber design made of a cylindrical DR composed of chemical liquids and analyzed the effects of the change in the dielectric properties of the DR on the absorption spectra numerically and experimentally [13]. Moreover, various absorber structures were designed by using micro-rod [17], micro-cylinder [18], vertical-square-split-ring [19], and two stacked square-shaped [20] DR structures with the temperature-sensitive InSb [17-19] and STO [20] materials. The effects of temperature-dependent changes in the dielectric properties of the InSb and STO materials on the absorption spectrum were investigated [17-20].

The absorbers based on DRs are generally excited by transverse electromagnetic (TEM) waves by using a free-space simulation setups [5, 9]. There are also reported studies where the structures are excited by transverse electric (TE) waves, which is specifically TE_{10} mode supported by rectangular waveguide simulation setups [13, 21]. Although several studies in the literature investigate the effects of simulation setups on the absorption, transmission, or reflection spectra for metallic resonators [23-26], no such study has been presented for DRs to the best of our knowledge.

In this study, several all-dielectric absorber structures composed of cylindrical-, elliptical-, square-, rectangular-, hexagonal-, and octagonal-shaped resonators are designed, and excited by using a rectangular waveguide simulation setup. The absorption mechanisms are discussed considering the electric and magnetic field distributions inside the resonators at their resonance frequencies. Moreover, sensitivity analyses are performed for each resonator geometry by changing the dielectric constant (ε_{diel}) and loss tangent ($\tan\delta_{diel}$) of the DRs. In addition to these analyses, the designed DRs are also excited by a TEM wave by using the free-space simulation setup formed by unit-cell boundary conditions (UC BCs). Herein, the effects of co- and cross-polarized components of *S*-parameters, and the periodicity of the unit-cell on the absorption spectra are investigated. Besides, the TE and TM mode analyses under the oblique incident wave are performed for all the designed DR-based absorber structures. Lastly, the amount of material used in each design is evaluated by calculating the volume value of each resonator geometry. In this sense, this study will contribute to the existing literature in terms of both the performed sensitivity analyses for the all-dielectric absorber based on DR having different resonator geometries and the investigations

TABLE I DESIGN PARAMETER VALUES OF THE DRS

	Design Parameters (mm)					
Resonator Structure	***r***	***r_x***	***r_y***	***a***	***b***	***h***
Cylindrical-shaped	14.5	—	—	—	—	11.5
Elliptical-shaped	—	15.5	11.5	—	—	11.5
Square-shaped	—	—	—	26.6	—	11.5
Rectangular-shaped	—	—	—	28	21	11.5
Hexagonal-shaped	—	—	—	16	—	11.5
Octagonal-shaped	—	—	—	11.5	—	11.5

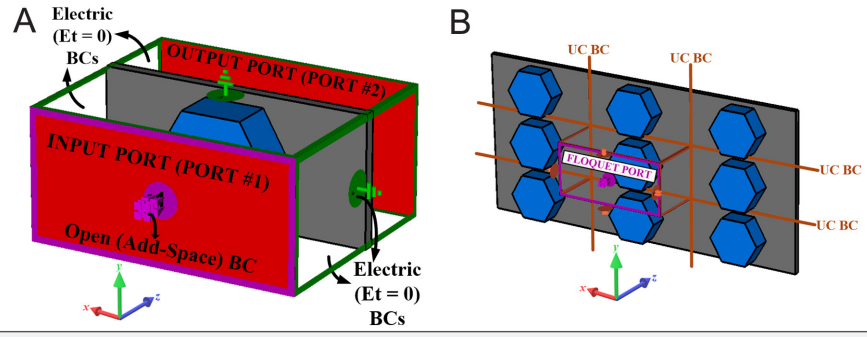

Fig. 2. (a) to (b) Simulation setup examples. (a) Waveguide simulation setup and (b) free-space simulation setup.

of the effects of the different BCs and excitation signals used in the simulation setups on the absorption spectra.

This article is an extended version of the national conference paper [21], which was previously published in Turkish, including additional analyses and discussions especially on free-space designs and comparisons.

II. DESIGN AND SIMULATION

The schematics and the design parameters of all-dielectric absorbers composed of DRs having cylindrical-, elliptical-, square-, rectangular-, hexagonal-, and octagonal-shaped geometry are presented in Fig. 1. In the designs, DRs have been placed on a polypropylene substrate with dielectric constant $\varepsilon_{PP} = 2.208$ and loss tangent

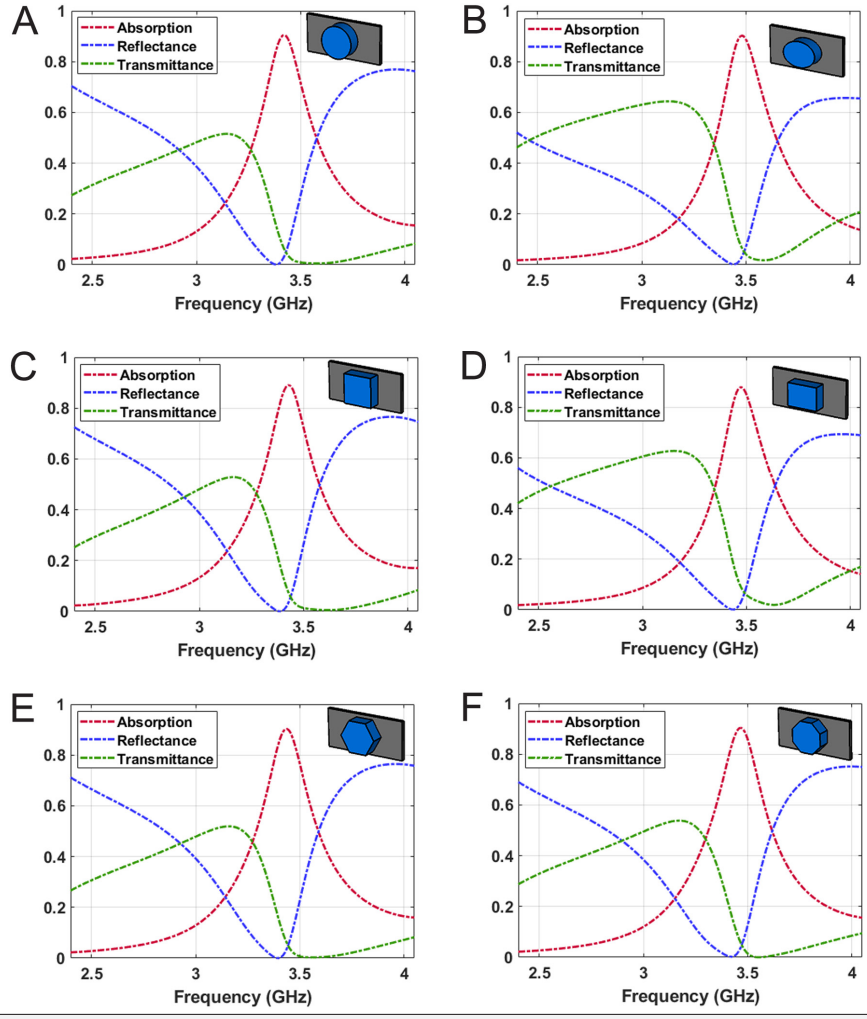

Fig. 3. (a) to (f) Absorption, reflectance, and transmittance plots for all-dielectric absorber structures composed of (a) cylindrical-, (b) elliptical-, (c) square-, (d) rectangular-, (e) hexagonal-, and (f) octagonal-shaped DRs.

$\tan\delta_{PP} = 0.000297$ values at 3.5 GHz [13]. The substrate dimensions are $L_x \times L_y \times t_{sub} = 72.136 \times 34.036 \times 3$ mm^3. At the starting point, the DRs have been formed by acetone as the dielectric material, having $\varepsilon_{diel} = 20.3$ ve $\tan\delta_{diel} = 0.042$ values at 2.45 GHz [27]. Acetone has been defined as a normal material in the CST Studio Suite® simulation environment. The dimensions of the resonators have been determined by parametrical numerical calculations so that the absorption resonance frequency is $f_0 \cong 3.4$ GHz. The values of the design parameters are presented in Table I.

In this study, all designs and simulations have been performed by using the frequency domain solver of Microwave Studio (MWS) in CST Studio Suite® (Dassault Systèmes, Vélizy-Villacoublay, France) software environment [28]. The simulations have been either performed with a rectangular waveguide setup or a free-space setup, or both depending on the analysis. Fig. 2A shows a representation of WR-284 waveguide-based simulation setup as an example. In the setup, the space surrounding the all-dielectric structure, which is defined by $\varepsilon_r = 1, \mu_r = 1$, has been ended by four electric ($E_t = 0$) boundary conditions (BCs) two each at x - and y -planes, and two open(add-space) BCs at z -planes. The structure under test has been excited by a y-polarized TE_{10} wave by two waveguide ports placed on the open(add-space) BCs. Since the propagation is assumed to be along the z -axis, the electrical field vector has only the y component, and the magnetic field vector has both x and z components. Owing to the sine function behavior of the magnetic field in TE_{10} mode, the x component of it is more dominant at the center of the waveguide, while the z component becomes more dominant towards the sides

TABLE II. ABSORPTION RESONANCE FREQUENCIES (f_0) AND ABSORPTION PEAK LEVELS FOR VARIOUS RESONATOR GEOMETRIES

Resonator Structure	f_0 (GHz)	Absorption Peak Level
Cylindrical-shaped	3.42	0.904
Elliptical-shaped	3.48	0.902
Square-shaped	3.43	0.891
Rectangular-shaped	3.47	0.879
Hexagonal-shaped	3.44	0.903
Octagonal-shaped	3.47	0.904

perpendicular to the x -axis [2]. In the designs, since the resonator structure is placed at the center of the waveguide's propagation plane, the x component of the magnetic field is evaluated to play an active role in the excitation of the all-dielectric absorber structures. On the other hand, Fig. 2B represents an example of a free-space simulation setup. This setup allows us to analyze co- and cross-polarized S-parameter components of the design under test. Moreover, in this study, we also aim to reveal the differences due to the BC difference. Therefore, all the designs presented in Fig. 1 have been analyzed with the free-space simulation setup once. As shown in Fig. 2B, in this setup, the space surrounding the structure, which is defined by $\varepsilon_r = 1, \mu_r = 1$, has been ended by four unit-cell BCs two each at x - and

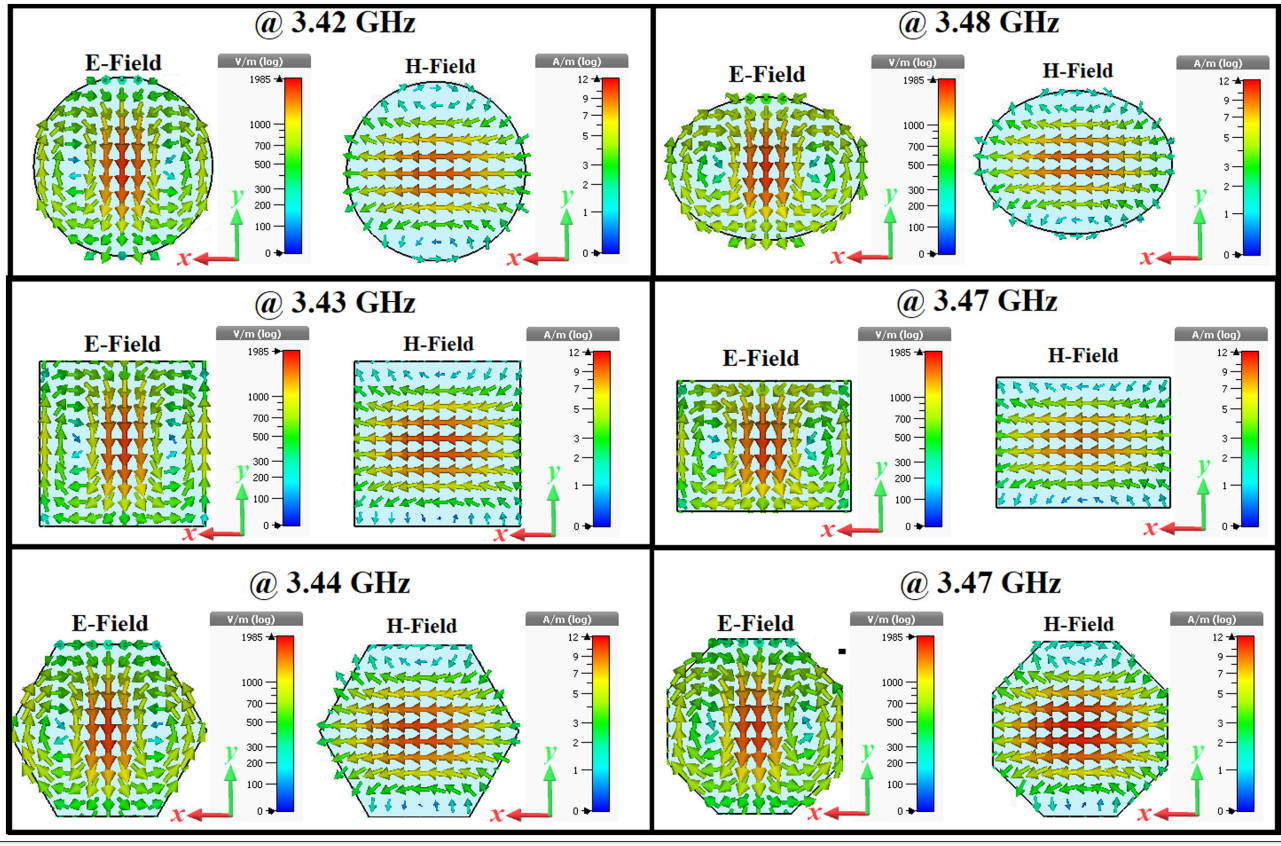

Fig. 4. E- and H-field distributions of cylindrical-, elliptical-, square-, rectangular-, hexagonal-, and octagonal-shaped DR geometries at their f_0 value. All plots are obtained for 60° phase angles.

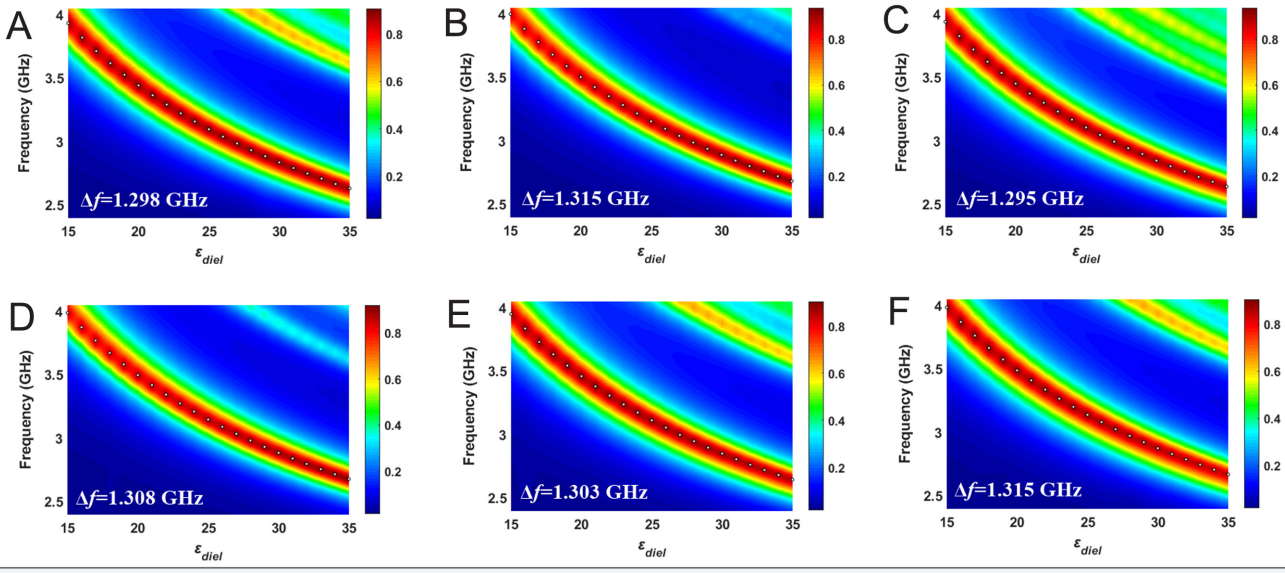

Fig. 5. (a) to (f) Two-dimensional absorption spectra of (a) cylindrical-, (b) elliptical-, (c) square-, (d) rectangular-, (e) hexagonal-, and (f) octagonal-shaped DR geometries for various ε_{diel} values. The white dots in the graphs demonstrate fundamental f_0 values.

y -planes and two open(add-space) BCs at z -planes. The structures are excited by Floquet ports supporting two transverse electromagnetic (TEM) wave modes (y -polarized and x -polarized) to investigate the co- and cross-polarized components of the *S*-parameters.

III. RESULTS

For the structures under investigation, absorption, reflectance, and transmittance plots are given in Fig. 3. Herein, absorption spectra are calculated by $Absorption = 1 - |S_{11}|^2 - |S_{21}|^2$ formula [13, 20] where $|S_{11}|^2$ and $|S_{21}|^2$ are defined as reflectance and transmittance, respectively [13]. In literature, it is stated that $|S_{11}|^2$ and $|S_{21}|^2$ may have co- and cross-polarized components [24, 29, 30]. Our further analyses that will come together with the free-space setup will show in the later parts that cross-polarized components of the *S*-parameters can be neglected for the designs under test in this study.

The plots in Fig. 3 show that both transmittance and reflectance take almost their minimum values at f_0, where the absorption becomes the maximum for all resonator geometries. For all absorber structures, f_0 and absorption peak level values are given in TABLE II. It has been observed that the absorption peak levels are over 0.85, and f_0 values are around 3.4 GHz for all cases.

To clarify the absorption mechanism, electric and magnetic field distributions have been plotted on the xy plane at the 60° phase angle for each resonator geometry at their f_0 values, and the results are given in Fig. 4. It has been observed for all resonator geometries

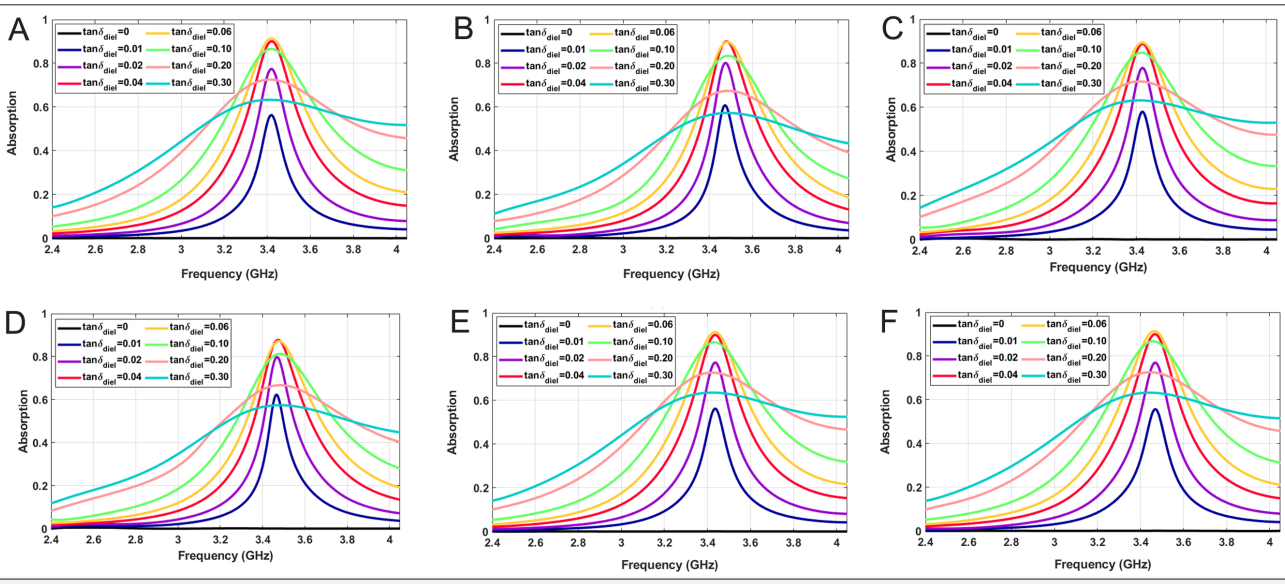

Fig. 6. (a) to (f) Absorption spectra of (a) cylindrical-, (b) elliptical-, (c) square-, (d) rectangular-, (e) hexagonal-, and (f) octagonal-shaped DR geometries for $\tan\delta_{diel}$ = 0, 0.01, 0.02, 0.04, 0.06, 0.1, 0.2, and 0.3 values.

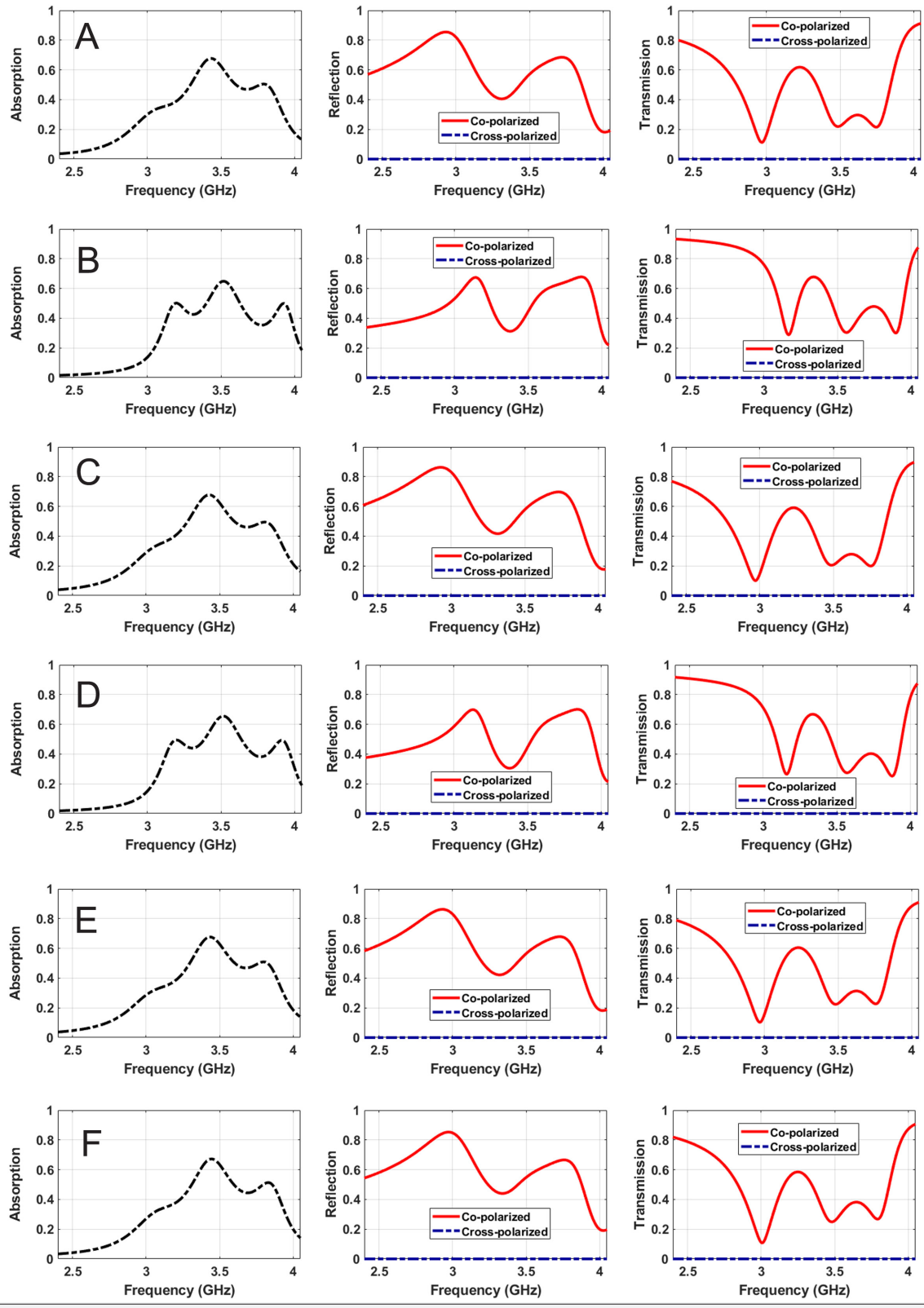

Fig. 7. (a) to (f) Absorption, co-polarized reflection and co-polarized transmission plots obtained by free-space simulation setup. (a) Cylindrical-shaped DR, (b) elliptical-shaped DR, (c) square-shaped DR, (d) rectangular-shaped DR, (e) Hexagonal-shaped DR, and (f) octagonal-shaped DR-based absorbers.

that the absorption peak occurs as the results of simultaneously excited electric and magnetic dipoles, which are perpendicular to each other, in the DR [5, 13].

On the other hand, to reveal the effect of resonator geometry on the sensitivity, $\tan\delta_{diel}$ is kept constant at 0.042, and ε_{diel} is changed from 15 to 35 with 1 step-size for all studied DR designs. The results are given in Fig. 5. The white dots in the plots demonstrate the fundamental f_0 locations, while Δf values denote the occurring amount of shifts at the f_0 in response to the change in the ε_{diel}. These Δf values are calculated by $\Delta f = f_{max} - f_{min}$ formula, where f_{min} and f_{max} indicate the f_0 values for $\varepsilon_{diel} = 35$ and $\varepsilon_{diel} = 15$, respectively. The following observations can be made from Fig. 5: (i) f_0 decreases with the increase of the ε_{diel} for all structures. (ii) The calculated Δf values are very close to each other for all resonator geometries under test. (iii) The absorption peak levels are almost independent of the geometry and take values over 0.85 for all ε_{diel} values. (iv) The absorption peaks for higher-order resonance modes become visible within the operating frequency band due to the decrease of f_0 in response to the increase in ε_{diel}. However, for higher-order resonance modes, while the absorption peak levels are evaluated to be relatively lower (with maximum value of 0.4) for elliptical- and rectangular-shaped DRs, they are relatively higher (with maximum value of 0.65) for cylindrical-, square-, hexagonal-, and octagonal-shaped DR structures.

Next, to expose the effect of $\tan\delta_{diel}$ on the sensitivity, ε_{diel} is kept constant at 20.3, and the absorption spectra are plotted for $\tan\delta_{diel} = 0$, 0.01, 0.02, 0.04, 0.06, 0.1, 0.2, and 0.3 values for all resonator geometries under interest as presented in Fig. 6. The plots in Fig. 6 show that in the beginning (i.e., just after $\tan\delta_{diel} = 0$ case), the absorption peak levels tend to increase in response to increase in the $\tan\delta_{diel}$. However, the absorption peak levels start to fall after their maxima at the specific $\tan\delta_{diel}$ values depending on the geometry. These specific $\tan\delta_{diel}$ values among the studied $\tan\delta_{diel}$ values are 0.04 for elliptical- and rectangular-shaped DRs and 0.06 for the remaining DR geometries. It is also observed that the rate of increase in the absorption peak levels is different for all resonator geometries. The fastest increase belongs to the elliptical-shaped resonator geometry (see Fig. 6B). On the other hand, the absorption bandwidths are observed to increase in response to the increase in $\tan\delta_{diel}$ for all resonator geometries under interest. Specifically, the absorption bandwidth is relatively larger in cylindrical-shaped resonator geometry.

To investigate the co- and cross-polarized S-parameters, the effects of using different boundary conditions and excitation signals, all the designed absorber structures have been once excited by TEM waves under the free-space simulation setup composed of UC BCs, as shown in Fig. 2B. Thereby, the absorption, co- and cross-polarized reflections, and co- and cross-polarized transmissions are numerically calculated and presented in Fig. 7. Taking the cross-polarization effects into account, the absorption spectra are calculated by $Absorption = 1 - |S_{11(co)}|^2 - |S_{11(cross)}|^2 - |S_{21(co)}|^2 - |S_{21(cross)}|^2$ formula, where $|S_{11(co)}|$, $|S_{11(cross)}|$, $|S_{21(co)}|$, and $|S_{21(cross)}|$ are magnitudes of co-polarized reflection, cross-polarized reflection, co-polarized

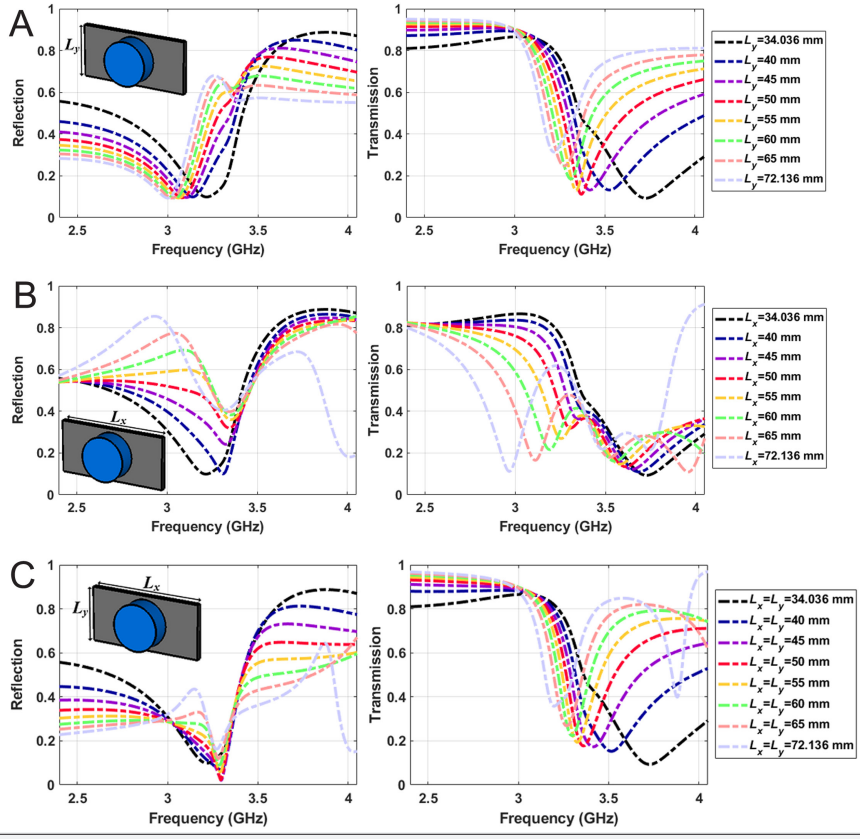

Fig. 8. (a) to (c) Co-polarized reflection and co-polarized transmission plots for cylindrical-shaped DR. (a) L_y = 34.036, 40, 45, 50, 55, 60, 65, and 72.136 mm while L_x = 34.036 mm. (b) L_x = 34.036, 40, 45, 50, 55, 60, 65, and 72.136 mm, while L_y = 34.036 mm. (c) L_x = L_y = 34.036, 40, 45, 50, 55, 60, 65, and 72.136 mm.

transmission, and cross-polarized transmission, respectively [24, 29, 30]. As shown in Fig. 7, the cross-polarized components of *S*-parameters are negligibly small for all resonator geometries. The maximum values of cross-polarized reflection and cross-polarized transmission have been found to be 8.36×10^{-5} (for rectangular-shaped DR geometry) and 1.81×10^{-5} (for hexagonal-shaped DR geometry), respectively, among the resonator geometries under investigation. The remaining values for the other cross-polarized

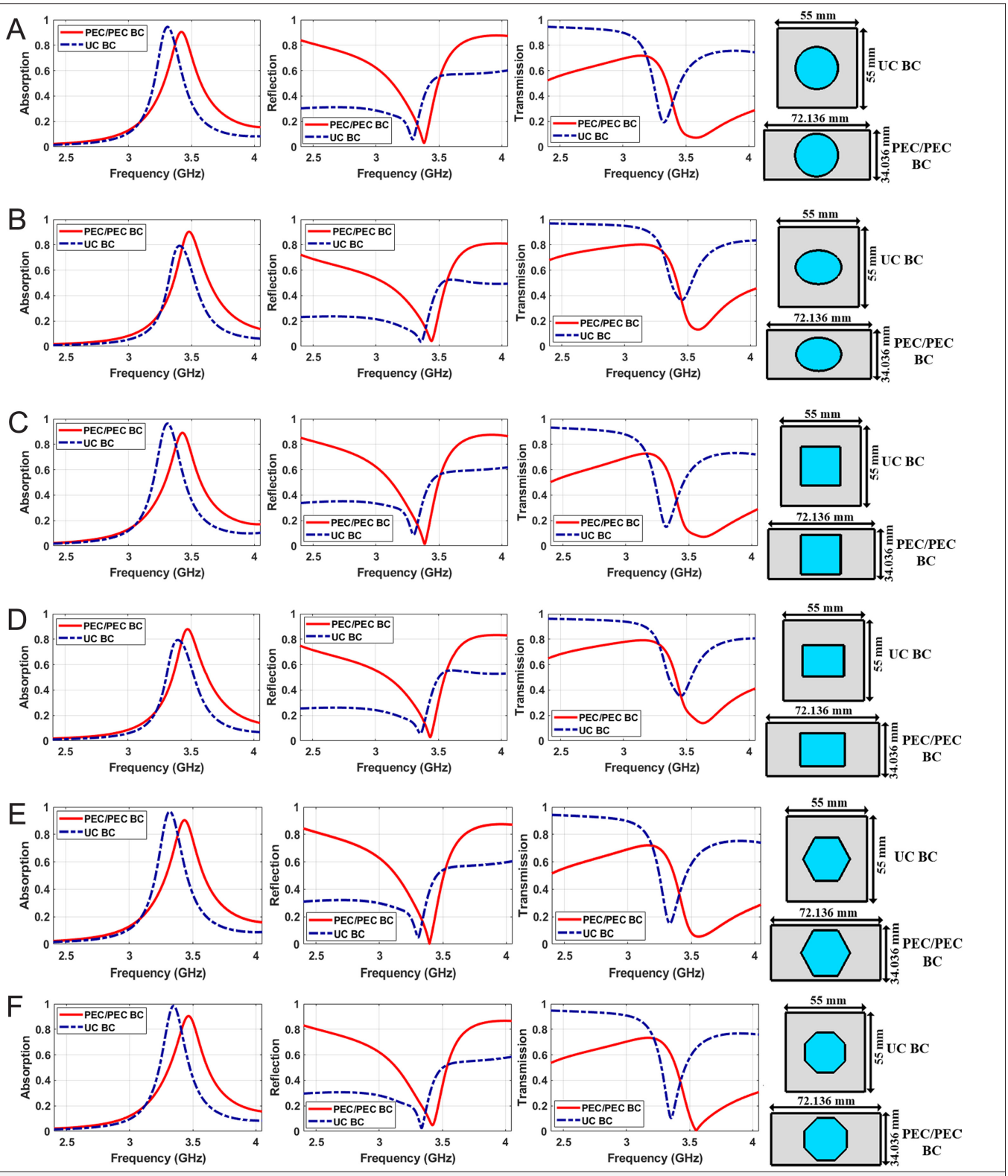

Fig. 9. (a) to (f) Absorption, co-polarized reflection, and co-polarized transmission plots of the (a) cylindrical-, (b) elliptical-, (c) square-, (d) rectangular-, (e) hexagonal-, and (f) octagonal-shaped DR-based absorbers.

terms in the operating frequency band are lower than these maximum values. Therefore, it has been evaluated for the designs studied in this work that the cross-polarized components of *S*-parameters are negligible in the absorption spectra calculation, and in this sense, using a waveguide test setup for the characterization is safe. On the other hand, Fig. 7 shows that the modes contributing to the absorption spectra are separated for all resonator geometries under investigation in the UC BC setup; therefore, the absorption spectra exhibit multiple absorption peaks with decreased amplitudes. It turns out that the simulation setup and excitation signal should be considered to observe a strong absorption spectrum while determining the design parameters of the all-dielectric absorber.

When studies in the literature are investigated, it has been observed that the resonance frequency of the modes contributing to absorption spectra not only depends on the resonator's design parameters but also on periodicity values of the all-dielectric absorber structures [5, 31, 32]. Therefore, to analyze the effects of the lateral and vertical periodicities (i.e., L_x and L_y, respectively) on the reflection and the transmission spectra, thus on the absorption spectra, a series of parametric analyses are performed. First, the L_x value is kept constant at 34.036 mm, and simulations have been performed for L_y =34.036, 40, 45, 50, 55, 60, 65, and 72.136 mm values. The related co-polarized reflection and transmission plots are given in Fig. 8A. Secondly, the L_y value is kept constant at 34.036 mm, and simulations have been performed for L_x =34.036, 40, 45, 50, 55, 60, 65, and 72.136 mm values. The related co-polarized reflection and transmission plots are given in Fig. 8B. Finally, the L_x and L_y parameters are changed simultaneously, and the simulations have been done for $L_x = L_y$ =34.036, 40, 45, 50, 55, 60, 65, and 72.136 mm values and related co-polarized reflection and transmission plots are presented in Fig. 8C. The results show that the changes in L_x and L_y both affect the reflection and transmission spectra. Since playing with the L_x and L_y leads to similar responses on the reflection and the transmission spectra of the DR-based absorbers under investigation, only the results of the cylindrical-shaped resonator-based absorber are presented here.

The results in Fig. 3 (regarding the waveguide simulation setup) are obtained with design parameter values that will provide almost maximum absorption peak value. Therefore, for a fair comparison, the design parameter values analyzed in Fig. 7 (regarding free-space simulation setup) have been revised in terms of only periodicity parameters without disturbing the DR geometries and dimensions to obtain the highest possible absorption peak levels using selected dielectric materials. For the final version of the revised structures, the periodicity of the unit-cell has been determined as 55×55 mm^2 by the parametrical analyses to obtain the highest possible absorption peak level. Consequently, the absorption, co-polarized reflection, and co-polarized transmission spectra are shown in Fig. 9. The results show that while the absorption peak level is slightly lower in waveguide simulations for the cylindrical-, square-, hexagonal-, and octagonal-shaped DR geometries, it is slightly lower in free-space simulations for elliptical-, and rectangular-shaped DR geometries. On the other hand, for all resonator geometries, f_0 values are lower for UC BCs. It is predicted that this is due to the excitation difference of the structure with TE_{10} mode under PEC/PEC BCs and with TEM wave mode under UC BCs. Since the guided wavelength is higher in the waveguide medium than in the free-space medium, the dimensions of the designed resonators for the waveguide become slightly larger electrically than the design for the free-space. Therefore, f_0 shifts to lower frequencies for the TEM wave excitation cases.

Moreover, the absorption performance of the cylindrical-, elliptical-, square-, rectangular-, hexagonal-, and octagonal-shaped DR-based all-dielectric absorber structures for transverse electric (TE) and transverse magnetic (TM) modes have been studied by

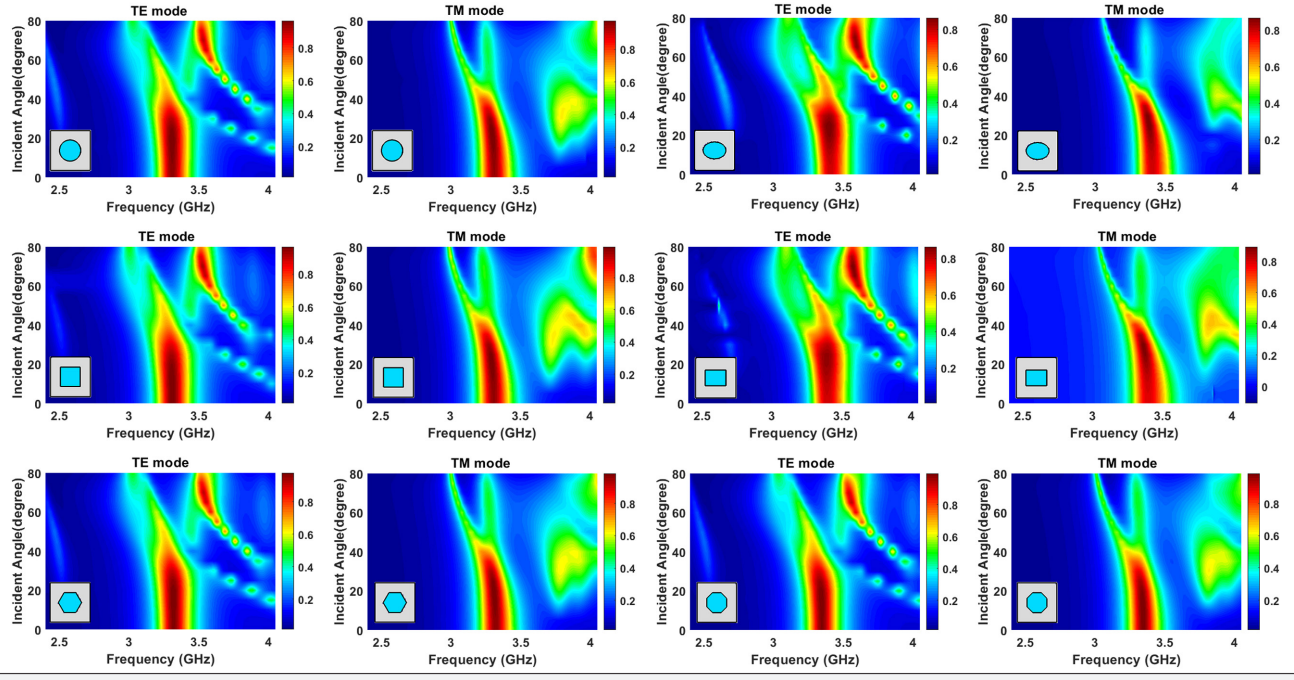

Fig. 10. Two-dimensional absorption plots for TE and TM modes of cylindrical-, elliptical-, square-, rectangular-, hexagonal-, and octagonal-shaped DR-based all-dielectric absorber structures under the oblique incident wave.

TABLE III. VOLUME VALUES OF VARIOUS RESONATOR GEOMETRIES.

DR Structure	Volume (mm³)
Cylindrical-shaped	7595.98
Elliptical-shaped	6439.87
Square-shaped	8075.88
Rectangular-shaped	6762
Hexagonal-shaped	7648.74
Octagonal-shaped	7343.69

using oblique incident waves. The incident angles of the waves are changed from 0° to 80° with 5° step sizes for both TE and TM modes. TE and TM mode analyses have been performed by using the free-space simulation setup for all-dielectric absorber structures having 55×55 mm² periodicities. 2D absorption plots for both TE and TM modes are plotted in Fig. 10. When the incident angle is less than 30° for TE mode, it has been observed that the absorption peak levels have too little change and remain over 0.8 for all the dielectric resonator geometries. As the incident angle increases, the effect of the magnetic field weakens, as stated in reference [12], resulting in a gradual decrease in absorption peak levels beyond the 30° incident angle. On the other hand, when the incident angle is under 35° for TM mode, the absorption peak levels have slightly changed for all the dielectric resonator geometries. It has been seen that over the incident angle of 35°, the absorption peak levels gradually decrease, and the electric and magnetic modes in the absorption spectra are split. In addition, parasitic absorption resonances have occurred with the increase in the incident angle at high frequencies for both TE and TM modes, as seen in Fig. 10.

Finally, the calculated volumes of the DRs are given in TABLE III. It has been observed that square-shaped DR has the highest volume, and elliptical-shaped DR has the lowest volume value. The lowest volumetric size of the elliptical-shaped DR in terms of the low amount of the substance under test may provide an advantage for a sensor application.

IV. CONCLUSION

In this study, the all-dielectric absorber designs composed of cylindrical-, elliptical-, square-, rectangular-, hexagonal-, and octagonal-shaped DR geometries have been studied. Their dependences on ε_{diel} and $\tan\delta_{diel}$, the unit-cell periodicity, and the excitation technique have been investigated in detail for the performance analyses. The obtained results show that the frequency shift at f_0 (i.e., Δf) is approximately 1.3 GHz (±15 MHz) for all DR geometries; therefore, the sensitivity on ε_{diel} is almost the same. On the other hand, the absorption peak levels of the higher-order resonance modes observed for higher ε_{diel} values are lower for elliptical- and rectangular-shaped DR geometries than cylindrical-, square-, hexagonal-, and octagonal-shaped DR geometries. Moreover, for all resonator geometries under test, the absorption peak levels increase up to a specific $\tan\delta_{diel}$ value and then decrease after this point. In addition, the free-space simulation setup analyses reveal that the cross-polarization components of the *S*-parameters are negligible. The periodicity value of the unit-cell and the boundary conditions in the excitation setup affect the absorption spectrum. The absorption peak levels for elliptical- and rectangular-shaped DRs are slightly higher in the simulations with the waveguide setup compared to the free-space setup. On the other hand, the absorption peak levels of the remaining DR geometries have higher values in the simulations with the free-space setup. For all DR geometries, the f_0 values are slightly lower in the free-space setup than in the waveguide setup. Furthermore, it has been established that the absorption spectra for the studied DR geometries are almost angle-independent under the incident angle of 30° and 35° for TE and TM modes, respectively. Lastly, it has been observed that DR-based absorbers with the same operating frequency, but different geometries possess distinct volume values. It is believed that the results of this study are important, especially for DR-based absorber designs for sensor applications.

Peer-review: Externally peer-reviewed.

Author Contributions: Concept – E.E.; Design – N.K., E.E.; Supervision – E.E.; Funding – E.E.; Materials – E.E.; Data Collection and/or Processing – N.K.; Analysis and/or Interpretation – N.K., G.T.S., E.E.; Literature Review – N.K., E.E.; Writing – N.K., E.E.; Critical Review – G.T.S., E.E.

Declaration of Interests: The authors have no conflict of interest to declare.

Funding: This study is supported by the Scientific and Technological Research Council of Türkiye (TÜBİTAK) (grant number 121R070).

REFERENCES

1. R. D. Richtmyer, "Dielectric resonators," *J. Appl. Phys.*, vol. 10, no. 6, pp. 391–398, 1939. [CrossRef]
2. D. M. Pozar, *Microwave Engineering*. Hoboken, NJ: John Wiley & Sons, Inc., 2011.
3. R. K. Mongia, and P. Bhartia, "Dielectric resonator antennas—A review and general design relations for resonant frequency and bandwidth," *Int. J. Microw. Mill.-Wave Comput.-Aided Eng.*, vol. 4, no. 3, pp. 230–247, 1994. [CrossRef]
4. L. Li *et al.*, "Achieving all-dielectric metamaterial band-pass frequency selective surface via high-permittivity ceramics," *Appl. Phys. Lett.*, vol. 108, no. 12, p. 122902, 2016. [CrossRef]
5. X. Liu, K. Fan, I. V. Shadrivov, and W. J. Padilla, "Experimental realization of a terahertz all-dielectric metasurface absorber," *Opt. Express*, vol. 25, no. 1, pp. 191–201, 2017. [CrossRef]
6. P. R. Meher, B. R. Behera, and S. K. Mishra, "Design and its state-of-the-art of different shaped dielectric resonator antennas at millimeter-wave frequency band," *Int. J. RF Microw. Comput. Aided Eng.*, vol. 30, no. 7, p. e22221, 2020. [CrossRef]
7. R. E. Jacobsen, A. V. Lavrinenko, and S. Arslanagić, "Electrically small water-based hemispherical dielectric resonator antenna," *Appl. Sci.*, vol. 9, no. 22, p. 4848, 2019. [CrossRef]
8. S. Jamilan, G. Semouchkin, and E. Semouchkina, "Analog of electromagnetically induced transparency in metasurfaces composed of identical dielectric disks," *J. Appl. Phys.*, vol. 129, no. 6, p. 063101, 2021. [CrossRef]
9. J. Zhao *et al.*, "Broadband microwave absorption utilizing water-based metamaterial structures," *Opt. Express*, vol. 26, no. 7, pp. 8522–8531, 2018. [CrossRef]
10. D. J. Seo, and J. Kyoung, "Shape dependence of all-dielectric terahertz metasurface," *Opt. Express*, vol. 30, no. 21, pp. 38564–38575, 2022. [CrossRef]
11. E. B. Whiting, S. D. Campbell, G. MacKertich-Sengerdy, and D. H. Werner, "Dielectric resonator antenna geometry-dependent performance tradeoffs," *IEEE Open J. Antennas Propag.*, vol. 2, pp. 14–21, 2021. [CrossRef]
12. J. Zhao, and Y. Cheng, "Temperature-tunable terahertz perfect absorber based on all-dielectric strontium titanate (STO) resonator structure," *Adv. Theor. Simul.*, vol. 5, no. 12, p.2200520, 2022. [CrossRef]
13. N. Karacan, and E. Ekmekci, "An all-dielectric microwave absorber composed of a dielectric hollow cylinder filled by chemical liquids and its application on sensing," Sens. Actuators A Phys., vol. 314, p. 112235, 2020. (https://doi.org/10.1016/j.sna.2020.112235), 2020.

14. J. Zi *et al.*, "Antireflection-assisted all-dielectric terahertz metamaterial polarization converter," *Appl. Phys. Lett.*, vol. 113, no. 10, p. 101104, 2018. [CrossRef]
15. Y. Cui, X. Wang, B. Ren, and Y. Jiang, "Polarization-controlled electromagnetically induced transparency analogue based on multipolar resonances," *Opt. Mater. Express*, vol. 12, no. 9, pp. 3738–3748, 2022. [CrossRef]
16. Q. Wang, Y. Liu, M. Zhang, X. Bai, and Z. Guo, "A simple dielectric resonator-based sensor for temperature measurement," *Results Phys.*, vol. 27, p. 104481, 2021. [CrossRef]
17. Y. Cheng, Z. Li, and Z. Cheng, "Terahertz perfect absorber based on InSb metasurface for both temperature and refractive index sensing," *Optical Materials*, vol. 117, p.111129, 2021. [CrossRef]
18. F. Chen, Y. Cheng, and H. Luo, "Temperature tunable narrow-band terahertz metasurface absorber based on InSb micro-cylinder arrays for enhanced sensing application," *IEEE Access*, vol. 8, pp.82981–82988, 2020. [CrossRef]
19. Z. Li, Y. Cheng, H. Luo, F. Chen, and X. Li, "Dual-band tunable terahertz perfect absorber based on all-dielectric InSb resonator structure for sensing application," *J. Alloys Compd*, vol. 925, p.166617, 2022. [CrossRef]
20. W. Li, and Y. Cheng, "Dual-band tunable terahertz perfect metamaterial absorber based on strontium titanate (STO) resonator structure," *Opt. Commun.*, vol. 462, p.125265, 2020. [CrossRef]
21. N. Karacan, G. Turhan-Sayan, and E. Ekmekçi, "Farklı dielektrik rezonatör geometrilerine sahip tamamı dielektrik soğurucu yüzey yapıları için hassasiyet analizleri," Elektrik-Elektronik ve Biyomedikal Mühendisliği Konferansı (ELECO 2022), Bursa, 2022.
22. P. D. Terekhov, V. E. Babicheva, K. V. Baryshnikova, A. S. Shalin, A. Karabchevsky, and A. B. Evlyukhin, "Multipole analysis of dielectric metasurfaces composed of nonspherical nanoparticles and lattice invisibility effect" *Phys. Rev. B*, vol. 99, no. 4, p. 045424, 2019. [CrossRef]
23. O. Turkmen, E. Ekmekci, and G. Turhan-Sayan, "Effects of using different boundary conditions and computational domain dimensions on modeling and simulations of periodic metamaterial arrays in microwave frequencies," Int. J. RF and Microwave Comp. Aid Eng., vol. 23, pp. 459-465, 2013. [CrossRef]
24. N. Karacan, E. Ekmekci, and G. Turhan-Sayan, "Response to "Comment on 'Sliding planar conjoined cut-wire-pairs: A novel approach for splitting and controlling the absorption spectra'" [J. Appl. Phys. 128, 126101 (2020)]," J. Appl. Phys., vol. 128, p. 126102, 2020. [CrossRef]
25. A. Muratoglu, and S. Uckun, "Application of several boundary conditions for bi-anisotropic metamaterial structures and investigation of electromagnetic response," EMC Türkiye 2015, the 3rd Electromagnetic Compatibility Conference (EMC, 2015). Istanbul, 2015.
26. M. Bakır, M. Karaaslan, F. Dincer, and C. Sabah, "Metamaterial characterization by applying different boundary conditions on triangular split ring resonator type metamaterials," *Int. J. Numerical Modelling*, vol. 30, no. 5, p. e2188, 2017. [CrossRef]
27. V. V. Komarov, *Handbook of Dielectric and Thermal Properties of Materials at Microwave Frequencies*. Norwood, USA: Artech House, 2012.
28. *CST STUDIO SUITE®, Dassault systèmes, the 3DEXPERIENCE® company*". Available: https://www.3ds.com/products/simulia/cst-studio-suite
29. Y. Li *et al.*, "Achieving wide-band linear-to-circular polarization conversion using ultra-thin bi-layered metasurfaces," *J. Appl. Phys.*, vol. 117, no. 4, p. 044501, 2015. [CrossRef]
30. H. Chen *et al.*, "Ultra-wideband polarization conversion metasurfaces based on multiple plasmon resonances," *J. Appl. Phys.*, vol. 115, no. 15, p. 154504, 2014. [CrossRef]
31. V. E. Babicheva, and J. V. Moloney, "Lattice effect influence on the electric and magnetic dipole resonance overlap in a disk array," *Nanophotonics*, vol. 7, no. 10, pp. 1663–1668, 2018. [CrossRef]
32. J. Tian, H. Luo, Q. Li, X. Pei, K. Du, and M. Qiu, "Near-infrared superabsorbing all-dielectric metasurface based on single-layer germanium nanostructures," *Laser Photonics Rev.*, vol. 12, no. 9, p. 1800076, 2018. [CrossRef]

Nezihe Karacan received her B.Sc. degree in electronics and communication engineering from Süleyman Demirel University, Isparta, Turkey in 2017. She is currently pursuing the Ph.D. degree in electrical and electronics engineering at Süleyman Demirel University, Isparta, Turkey. She has served as a Research Assistant in Department of Electrical and Electronics Engineering at Süleyman Demirel University since 2022. Her research interests include absorbers, dielectric resonators, and sensors.

Gönül Turhan-Sayan received her B.S. and M.S. degrees from the Middle East Technical University (METU), Ankara, Turkey in 1979 and 1981, respectively, and her Ph.D. degree from the Ohio State University (OSU), Columbus, Ohio, USA in 1988, all in electrical engineering. At the OSU, she studied as a Fulbright scholar and worked for the ElectroScience Laboratory as a graduate research associate from 1984 to 1988.

Dr. Turhan-Sayan was a consultant for the Electromagnetics and Optics Divisions of the Battelle Memorial Institute, Columbus, Ohio, USA from 1988 to 1992. She has been a faculty member at METU since 1992, being a Full Professor since 2003. She served as the chairperson of the Electrical and Electronics Engineering Department in 2013-2016 and as the Vice President of METU in 2016-2017 overseeing the university's research programs.

Professional interests of Prof. Turhan-Sayan are focused in applied electromagnetics, photonics and radar signal processing including electromagnetic target recognition, ultra-wide band radar systems with GPR applications, metamaterial design in microwave, terahertz and infrared regions, multi-purpose metamaterial sensors, surface plasmon resonance sensors and distributed fiber optical sensors.

Evren Ekmekçi received his B.Sc. degree in electronics and communication engineering from Süleyman Demirel University, Isparta, Turkey in 2002 and his Ph.D. degree in electrical and electronics engineering from the Middle East Technical University, Ankara, Turkey in 2010. Dr. Evren Ekmekçi was a Visiting Scholar in Physics Department at Boston University, Boston, MA for one year from August 2009 to August 2010. He is currently a Professor in the Department of Electrical and Electronics Engineering, Süleyman Demirel University, Isparta, Turkey. His research interests include applications of metamaterials, dielectric resonators, and antennas.